THE THERMAL CONDUCTIVITY OF GRANULAR AND WEAKLY SINTERED MATERIALS

G. N. Dul'nev, Yu. P. Zarichnyak, and B. L. Muratova

UDC 536.2

We propose a new stable model of a granular or sintered material in a form with a second-order structure, with mutually penetrating components. We derive the functional relationships for the calculation of the coefficients of generalized conductivity* for the granular and sintered materials.

1. Discussion of the Need for the Construction of a New Model of Granular Systems

Numerous books, surveyed in [1-6], have been devoted to a study of the process of heat transfer in granular systems. The adequacy of the physical model and of the real system are usually evaluated on the basis of the extent to which the calculation results coincide with the experimental data. However, agreement with experiment, despite its value, is by no means a definitive criterion for the quality of a given model or calculation scheme, since the comparison is not always sufficiently extensive to cover the entire possible range of variation in the significant parameters. The testing of any given formula by other researchers with different materials in another range of variation for the determining parameters, on occasion, reveals substantial differences between the calculation results and those of the experiment.

Satisfactory agreement in limited comparison with experiment may be a random occurrence, or it may be explained by the mutually offsetting effect of individual defects within the model, or it may be a consequence of an inaccuracy in the mathematical conversions. In addition to comparing the calculation results with the experiment – an absolutely mandatory requirement – we should devote some attention to the internal adequacy of the model. With regard to granular systems, the internal adequacy of the model apparently should be understood to refer to the extent to which the model corresponds to the real structure of the system, its physical stability, and its isotropicity.

One method of determining the internal adequacy of a model is the testing of the working formula derived from that model on the limit transitions. In the limiting cases, with a porosity of $m_p \simeq 0.26$ (models with a tetrahedral packing) and $m_p \simeq 0.47$ (models with cubic packing), many of the working formulas lead to physically absurd results. Thus, for example, the functional relationships for the calculations of thermal conductivity [7, 8] for $m_p = 0.26$ yield a value of $\lambda = \infty$ for the effective thermal conductivity; in [4, 7, 9-12], as $m_s \to 1$, we are told that $\lambda < 0$ or $\lambda = 0$, or we are given a positive but physically invalid result. For the case in which $\lambda_p/\lambda_s = 1$ we should expect $\lambda = \lambda_s = \lambda_p$. However, the working formulas from [4, 7, 9, 11-13] do not yield the anticipated result. All of the formulas derived from models of noncontacting inclusions of any shape, distributed through the matrix, with $\lambda_p = 0$ yield $\lambda = 0$, which contradicts the experimental data. Let us draw attention to another two important factors – the isotropicity of the model and its physical stability, factors virtually not touched upon in the above-cited surveys [1-6]. The random nature of the structure in real granular systems determines the isotropicity of their properties. This fact must be borne in mind in devising ordered models of a granular system, in choosing the form of its symmetry, and in selecting the "elementary cell," for which we undertake the mathematical description of the process within the volume of that cell. Isotropicity for the properties of the granular system can be achieved in

*The coefficient of generalized conductivity will subsequently be understood to refer to any of the coefficients of thermal or electrical conductivity, to the permittivity or to magnetic permeability.

Institute of Precision Mechanics and Optics, Leningrad. Translated from Inzhenerno-Fizicheskii Zhurnal, Vol. 16, No. 6, pp. 1019-1028, June, 1969. Original article submitted June 24, 1968.

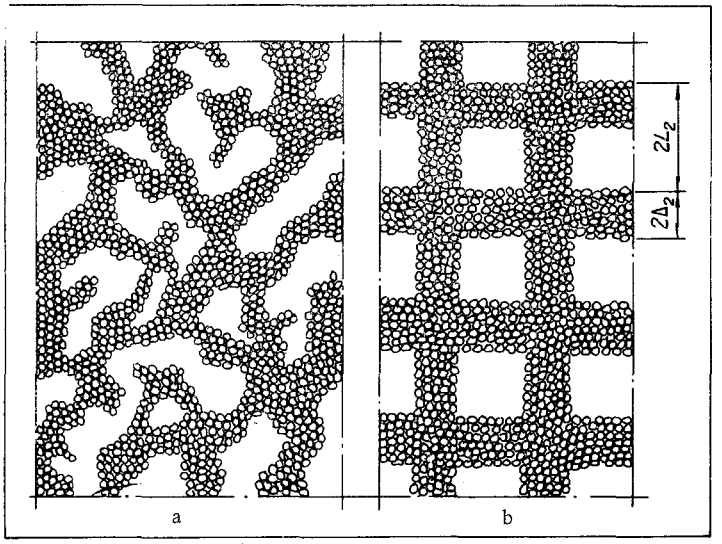

Fig. 1. Diagram relating to the new model of the granular system: a) schematic representation of the structure of real granular material; b) stable model with spherical grains in the form of a complex second-order structure.

two ways: a) by the construction of an isotropic elementary cell; b) by the use of an anisotropic elementary cell, with subsequent analytical averaging of its properties in all directions.

2. The Stability of Models of Granular Systems

The most frequently used models of granular systems in the form of spherical particles with any ordered packing are strictly stable only for a single specific value of the component volume concentration (for example, $m_p \simeq 0.26$ for tetrahedral packing, $m_p \simeq 0.47$ for cubic packing, etc.). It is impossible to substantiate the stability of models of granular systems in the form of noncontacting inclusions of any shape (the solid component), distributed within the gas component [3, 7, 8, 10-13]. These models are suitable, more likely, for the description of aerosol structure (smokes and fogs).

We can cite the following reasons which, in our opinion, partially explain the stability of real monodisperse granular systems, when their porosity differs from the theoretical values: the combined packing (individual segments of the system are formed by various types of packing); deviations in the shape of real particles from that of the simplest geometric figures and the existence of microirregularities; the existence of a more complex system structure formed by segments with a dense grain packing and a space lattice of larger voids, penetrating the entire volume of the granular system.

It is natural to assume that in real granular materials all of the above-enumerated three factors apply.

1) The presence of combined packing (a combination of tetrahedral and cubic packing, or others) provides a substantiation of the stability of a model with spherical grains only for a narrow range of variation in porosity from $m_p \simeq 0.26$ to $m_p \simeq 0.47$. With a porosity of $m_p > 0.47$ no manner of ordered packing for the spherical particles in contact results in a physically stable model and the separate grains seemingly float in space.

2) Measurements of porosity for real granular materials with grains of various configurations (spheres, cylinders, cubes, ellipsoids of revolution, etc.) demonstrated that the porosity of such systems depends weakly on particle shape, and the microirregularities have virtually no effect on the porosity of the granular system [1, 7]. Consequently, deviations in grain shape from the spherical and the existence of microirregularities cannot serve as a basis for the stability of granular systems in the case of high porosity.

3) Direct observation of various granular systems by means of a binocular microscope makes possible schematic two-dimensional representation of structure (see Fig. 1a). It can be seen that the granular system is formed by a "skeleton," consisting of a disordered but relatively dense grain packing (a first-order structure) and larger voids, penetrating the skeleton and forming – together with the skeleton – a

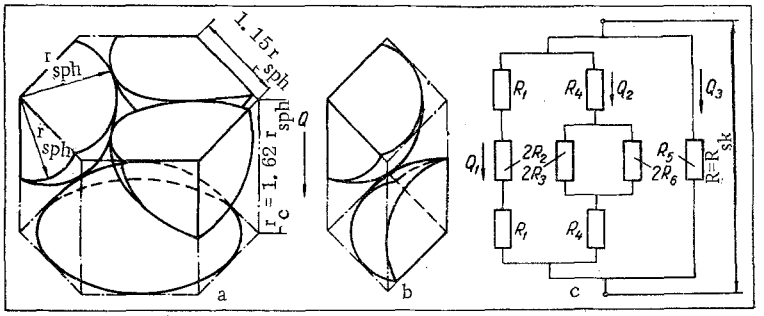

Fig. 2. Investigation of heat transfer in the elementary cell: a) selected form of the elementary cell in tetrahedral packing; b) the one-third of the elementary cell under consideration; c) circuit connecting the thermal resistances of the individual parts of the cell.

structure with mutually penetrating components (a second-order structure). Such a structure can actually exhibit stability over the entire range of variation in porosity.

The first stable models suitable for description of granular-system structures were proposed in [14-16] and represented modifications of structure models with mutually penetrating components. The shortcoming of these models is the rough schematization of the clearance geometry between the grains and the fact that the grain shape is a function of porosity, which resulted in substantial distortion of grain shape for high porosities $m_p > 0.7$).

The effort to eliminate the drawbacks in the models [14-16] lead to the development of a new stable model for granular and sintered materials, based on the important assumption that the effective thermal conductivities of systems with disordered and ordered skeletons are equal to each other, provided the component volume concentrations and their coefficients of thermal conductivity are, respectively, equal. The model of the granular system in the form of a second-order structure is stable over the entire range of variation for the porosity of real granular systems and because of cubic symmetry it is isotropic.

A general method was proposed in [14] to determine the effective thermal conductivity of higher-order structures by successively reducing these to first-order structures. We will apply this method to the problem under consideration. In the first stage, we determine the thermal conductivity λ_{sk} of the skeleton from the known values for the thermal conductivity λ_i of the components, the porosity m_{sk}, and the nature of its structure, i.e.,

$$\lambda_{sk} = f_1(\lambda_s, \lambda_p, m_{sk}). \tag{1}$$

The form of the functional relationship (1) is governed by the nature of the packing and grain shape. If the skeleton thermal conductivity for the first-order structure is determined (we will show how this is to be done later on), the effective thermal conductivity for the entire granular system (the second-order structure) is calculated from the formulas for structures with mutually penetrating components [14], and namely

$$\lambda = \lambda_{sk}\left[c_2^2 + \nu_2(1-c_2)^2 + \frac{2\nu_2 c_2(1-c_2)}{\nu_2 c_2 + (1-c_2)}\right], \quad \nu_2 = \frac{\lambda_p}{\lambda_{sk}}. \tag{2}$$

Here $c_2 = \Delta_2 / L_2$ is the geometric parameter of the model, associated with the volume concentration m_{p2} of the gas component in the second-order structure by the equation

$$m_{p2} = 2c_2^3 - 3c_2^2 + 1, \tag{3}$$

whose solution is given in [17, 18].

The problem can be regarded as solved, if we know the form of the functional relationship (1) and the method of determining the porosity (m_{sk}) of the first-order structure and (m_{p2}) of the second-order structure. If we denote the overall porosity m_p, it is not difficult to establish the relationship between m_p, m_{sk}, and m_{p2}, i.e.,

$$m_{p2} = (m_d - m_{sk})(1 - m_{sk})^{-1}. \tag{4}$$

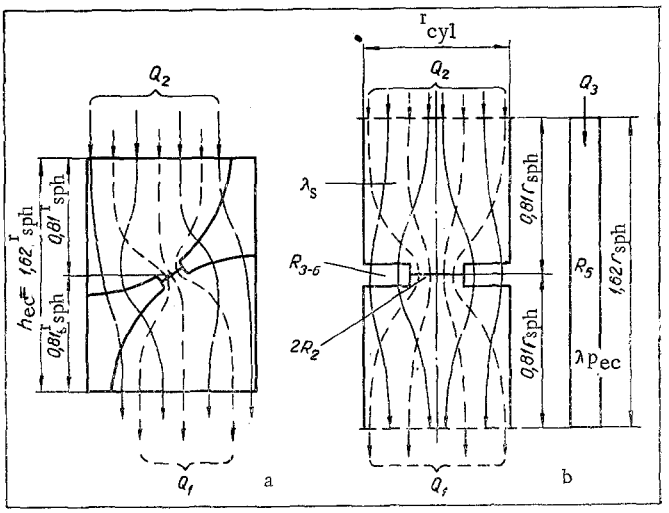

Fig. 3

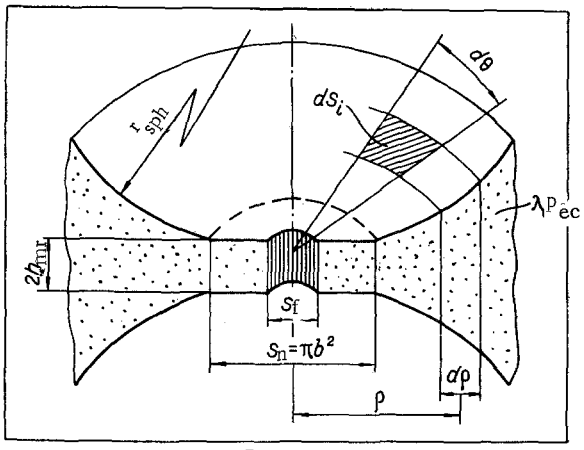

Fig. 4

Fig. 3. Schematic representation of streamline distribution for flows Q_1 and Q_2: a) in the longitudinal cross section of the elementary cell, through the point of contact; b) in the thermal model.

Fig. 4. Diagram for the calculation of the thermal resistance R_5 (schematic representation of space between grains).

Testing the functional relationship (2) for passage to the limit leads to obvious results: 1) $m_p = 1$, $m_{p2} = 1$, $\lambda = \lambda_p$; 2) $m_p = m_{sk}$, $m_{p2} = 0$, $\lambda = \lambda_{sk}$; 3) $\nu_2 = 1$, $\lambda = \lambda_{sk} = \lambda_p$. Let us now turn to the determination of the coefficient of thermal conductivity for the skeleton.

3. Thermal Conductivity of the Skeleton

Let us assume that the skeleton is formed of grains of the simplest spherical shape, with tetrahedral packing. We will examine the transfer of heat in the skeleton, but not through the entire volume of the skeleton; rather, we will consider the "elementary cell," whose shape in the tetrahedral packing depends on the chosen direction of the heat flow. In the tetrahedral packing, because of isotropicity, all directions are equivalent and we will therefore examine the transfer of heat in the direction in which the elementary cell has the form of a proper hexagonal prism (Fig. 2a). The bases of the prism in this case are isothermal, while the side facets are adiabatic planes. The axial symmetry of the elementary cell enables us to study the transfer of heat in one third of the cell (Fig. 2b). The circuit showing the connection of the heat resistances for the individual segments of the elementary cell is shown in Fig. 2c and corresponds to the following proposed physical pattern of the heat-flow distribution. The transfer of heat between the isothermal bases is accomplished by means of three flows. The flow Q_1, passing exclusively through the solid component (see Fig. 3a) enters into one sixth of the spherical grain through the area $S_{in} = 1/3\pi r_{sph}^2$, passing through the constriction formed by the point of contact with the area $S_f = \pi a^2$, and then passing through the second one sixth portion of the sphere, it reaches the bases. The flow Q_2 enters the elementary cell through the same area S_{in} and, passing successively through the solid particle, the annular gas space between the grains, and the other particle, it reaches the bases of the prism. The flow Q_3 passes through the elementary cell, following the open pores. The thermal resistances of the individual segments of the model are found in approximate terms. For this we replace the individual segments of the elementary cell by bodies of simpler shape, and namely: we replace the spherical part with cylinders having a height of 0.81 r_{sph} with the same values for the areas of the inlet and points of contact, and the open pores on the remaining area are shown in the form of a flat wall (Fig. 3b). Let us examine the means of determining individual thermal resistances for such a model.

The expression for the thermal resistance of the cylinder with an axial point of entry is taken from [14], i.e.,

$$R = R_{10}\Phi, \quad R_{10} = \frac{0{,}81r_{sph}}{\lambda_s \pi a^2} = \frac{0{,}81}{\lambda_s \pi y^2 r_{sph}}, \quad y = \frac{a}{r_{sph}},$$

$$\Phi = \Phi\left(\sqrt{3}\,y, \frac{r_{cyl}}{h_{ec}}\right) = 1 - 16\pi^{-2}\sum_{n=1}^{\infty} I_1\left(n\pi\sqrt{3}\,y\frac{r_{cyl}}{h_{ec}}\right) n^{-2} I_1^{-1}\left(n\pi\frac{r_{cyl}}{h_{ec}}\right)\left[I_1\left(n\pi\frac{r_{cyl}}{h_{ec}}\right)K_1\left(n\pi\sqrt{3}\,y\frac{r_{cyl}}{h_{ec}}\right)\right. \quad (5)$$

$$-K_1\left(n\pi\frac{r_{cyl}}{h_{ec}}\right)I_1\left(n\pi\sqrt{3}y\frac{r_{cyl}}{h_{ec}}\right)\Big], \quad n=2m+1,\ m=0,\ 1,\ 2,\ldots \tag{6}$$

The function Φ is related to the determining parameters y and r_{cyl}/h_{ec} in graphical form in [14]. For small points of contact ($y \leq 5\cdot10^{-2}$) the function Φ can be approximated by the relationship

$$\Phi\left(\sqrt{3}y,\ \frac{r_{cyl}}{h_{ec}}\right)\simeq 1{,}2y. \tag{7}$$

The thermal resistance R_4 of the cylinder to the flow Q_2 entering the gas space through the annular spot is determined approximately in analogy with (5) in the form $R_4 = R_{40}\varphi$. The function $\varphi(\sqrt{3}y,\ r_{cyl}/h_{ec})$ characterizes the change in the resistance R_{40} as a result of current leakage through the entire cross section. For this we present the heat flow q flowing through a uniform cylinder of length L between the isotherms T_2 and T_1 in the following form (the superposition principle):

$$q = q_1 + q_2 = \sigma(T_2 - T_1), \tag{8}$$

and here $q_1 = \sigma_1(T_2 - T_1)$ is the flow of heat passing through the cylinder with the axial point of entry and adiabatic walls; $q_2 = \sigma_2(T_2 - T_1)$ is the flow of heat passing through the cylinder with the annular point of entry. Since the temperature difference $(T_2 - T_1)$ is identical, it follows from (8) that

$$\sigma = \sigma_1 + \sigma_2. \tag{9}$$

The conductivity of the individual segments is expressed in the form

$$\sigma = \lambda_s S_c L^{-1};\ \sigma_1 = \lambda_s S_f L_1^{-1};\ \sigma_2 = \lambda_s S_{sk} L_2^{-1}. \tag{10}$$

Having presented the effective length of the streamlines in the form $L_1 = L\Phi$ and $L_2 = L\varphi$, with consideration of (8)-(10) it is not difficult to find the relationship between the functions Φ and φ

$$\varphi = \frac{S_{cyl} - S_f}{S_{cyl} - S_f\Phi^{-1}} = \frac{1 - Y^2}{1 - Y^2\Phi^{-1}} \tag{11}$$

and to obtain the expression for the thermal resistance R_4

$$R_4 = R_{40}\varphi = \frac{0{,}81 r_{sph}}{\lambda_s\pi(r_{cyl}^2 - a^2)}\varphi = \frac{2{,}43}{\lambda_s\pi(1-3y^2)r_{sph}}\varphi. \tag{12}$$

The thermal contact resistance is determined from the formula for a flat wall, i.e.,

$$R_2 = \frac{h_{mr}}{\lambda_s S_{mc}} = \frac{\bar{h}}{\lambda_s\pi y^2 r_{sph}}. \tag{13}$$

The thermal resistance of the space between the grains is made up of the parallel-connected resistance R_3 of the spherical portion and the resistance R_6 of the flat microclearance of height h_{mr} in the region of nominal contact with the area $S_{mc} = S_n - S_f$

$$R_6 = \frac{h_{mr}}{\lambda_p S_{mc}} = \frac{\bar{h}}{\lambda_p\pi(z^2 - y^2)r_{sph}},\quad z = \frac{b}{r_{sph}}. \tag{14}$$

The nominal contact area $S_n = \pi b^2$ is usually evaluated on the basis of the Hertz formula for elastic spheres [6, 7]. The actual contact area depends on the magnitude of the external load, the geometry of the microroughnesses, and the strength characteristics of the solid components. In the case of free flow $S_f/S_n = 1\cdot10^{-2}$-$1\cdot10^{-5}$. The height of the microroughnesses for granular materials with an untreated surface generally is $h_{mr}/r_{sph} = 1\cdot10^{-2}$-$1\cdot10^{-4}$ [6, 7].

The thermal resistance R_3 of the spherical portion of the space is evaluated in approximate terms, dividing this space concentrically with annular adiabatic surfaces, as shown in Fig. 4, i.e.,

$$R_3 = \frac{1}{\sigma_3},\quad \sigma_3 = \int_\varphi\int_\rho d\sigma_3 = \int_0^{2\pi}\int_b^{r_{cyl}}\frac{\lambda_p\rho d\rho d\theta}{r_{sph} + h_{mr} - \sqrt{r_{sph}^2 - \rho}},$$

$$R_3 = \frac{1}{2\pi\lambda_p r_{sph}}\left[0{,}815 - \sqrt{1-z^2} + (1+\bar{h})\ln\frac{1+\bar{h}-0{,}815}{1-\bar{h}-\sqrt{1-z^2}}\right]^{-1}. \tag{15}$$

The thermal resistance R_5 of the open gas pores is given approximately in the form

$$R_5 = \frac{h_{ec}}{\lambda_p} \frac{3}{S_{tc} - \pi r_{sph}^2}. \tag{16}$$

Having determined the values of the thermal resistances for the separate parts of the elementary cell, we can derive the expression for the equivalent or effective thermal resistance R of the entire circuit. The thermal resistance of the elementary cell can be expressed differently, in terms of its geometry and its effective thermal conductivity, i.e.,

$$R_{cyl} = \frac{3h_{ec}}{\lambda_{cyl} S_{tc}} = \frac{3h_{ec}}{\lambda_{cyl} S_{tc}}. \tag{17}$$

Having equated the expressions for the thermal resistances of the elementary cell, calculated in accordance with the circuit shown in (Fig. 2) and on the basis of (17), let us determine the effective thermal conductivity of the elementary cell and, consequently, of the entire skeleton. The theoretical formula has the form

$$\frac{\lambda_{sk}}{\lambda_s} = \frac{2.24y^2}{0.81\Phi + \bar{h}} + 2.24\left[\frac{\bar{h}}{\nu_2(z^2 - y^2) + 2\bar{h}\psi} + \frac{2.43\varphi}{1 - 3y^2}\right]^{-1} + 8.9\cdot 10^{-2}\nu_2,$$

$$\psi = 0.815 - \sqrt{1 - z^2} + (1 + \bar{h}) \ln \frac{1 + \bar{h} - 0{,}815}{1 + h - \sqrt{1 - z^2}}, \quad \nu_2 = \frac{\lambda_p}{\lambda_s} \tag{18}$$

and satisfies the passage to the limit.

4. The Thermal Conductivity of the Component Filling the Pore

If the pores are filled with the gas component, its thermal conductivity is composed of the molecular and the radiation components and depends on the pore size [17], i.e.,

$$\lambda_p = \lambda_{pm} + \lambda_{pr} \tag{19}$$

The molecular component λ_{pm} is calculated [10] on the basis of the following formula:

$$\lambda_{pm} = \lambda_0 [1 + B/H\delta_i]^{-1},$$
$$B = 4\gamma(1 + \gamma)^{-1}\, \mathrm{Pr}^{-1}(2 - a_1)\, a_1^{-1}\, \Lambda_\infty \left(1 + \frac{S}{T}\right)^{-1} H_0. \tag{20}$$

The average pore size in the skeleton (the first-order structure) is defined as the mean integral thickness of the state between the grains on the area $\pi(r_{cyl}^2 - a^2)$ (see Fig. 4) and is equal to $\delta_1 = (0.09 + \bar{h})$.

By examining the geometry of the elementary cell in a second-order structure, we can find the function with which to calculate the average pore size in the second-order structure. From visual observations of various granular materials we see that $2d < \Delta_2 < 5d$ (see Fig. 1b). For the calculations we will take the average value $\Delta_2 = 3d$, in which case

$$\delta_2 = 2(L_2 - \Delta_2) = 6d(c_2^{-1} - 1). \tag{21}$$

To evaluate the radiation component in the first-order structure (the skeleton) we will use [1] the following relationship:

$$\lambda_{l_1} = 2\varepsilon_1^2 C_0 T^3 \delta_1. \tag{22}$$

In calculating the radiation component in the second-order structure we will use the method proposed in [19]. We will regard the entire granular system as a continuous isotropic medium with an integral absorption coefficient α, a thickness l, and a skeleton emissivity of $\varepsilon_2 \simeq 1$. In this case,

$$\lambda_{l_2} = 0.3\left(\frac{T}{100}\right)^3 \frac{Y}{\alpha}. \tag{23}$$

The parameter Y can be evaluated with provision for the attenuation of radiation flux by using the graphical relationship $Y = f(\tau, \varepsilon_2)$, given in [19]. For $\tau > 10$, which is characteristic of most granular materials whose porosity $m_p < 0.8$, we can assume $Y \simeq 1$.

Comparison of the theoretical values for the effective thermal conductivity of granular systems over a broad range of variation in the determining parameters (λ_s, λ_p, m_p, T, H) with experiment confirms the possibility of using the new model and the functional relationship (18) to predict the properties of granular systems. A detailed analysis of (18) and a detailed comparison of the calculation results with experimenta data will be published in subsequent reports.

NOTATION

m_p	is the total volume concentration of the gas component in the pores of the granular system;
λ	is the effective thermal conductivity;
λ_p	is the thermal conductivity of the gas component in the pores;
λ_s	is the thermal conductivity of the solid component;
λ_{sk}	is the thermal conductivity of the skeleton;
m_{sk}	is the volume concentration of the gas component in the skeleton (first-order structure);
m_{p2}	is the volume concentration of the gas component in the second-order structure;
Δ_2	is half the thickness of the skeleton link in the second-order structure;
L_2	is the dimension of the elementary cell in the second-order structure;
r_{sph}	is the radius of the spherical grains;
a	is the radius of the point of actual contact;
$r_{cyl} = r_{sph}/\sqrt{3}$	is the radius of the cylinder whose cross-sectional area is $\pi r_{sph}^2/3$;
I_1	is the first-order Bessel function of the first kind and of imaginary argument;
K_1	is a first-order McDonald function;
h_{mr}, $\bar{h} = \bar{h}_{mr}/r_{sph}$	are, respectively, the absolute and relative heights of the microroughness;
b	is the radius of the nominal contact area;
S_{tc}	is the area of the elementary cell, equal to the area of the hexagon described about the grain;
$h_{ec} = 1.62 r_{sph}$	is the height of the elementary cell;
λ_{pm} and λ_{pr}	are, respectively, the molecular and radiation components of the coefficient of thermal conductivity in the pores;
λ_0	is the thermal conductivity of the gas at atmospheric pressure, H_0 = 760 mm Hg;
σ_i	is the average dimension of the i-th pore;
$\gamma = c_p/c_v$	is the ratio of isobaric and isochoric heat capacities;
Pr	is the Prandtl number for the gas in the pores;
a_1	is the accommodation factor of the gas;
Λ_∞	is the molecular mean free path of the gas at an infinitely high temperature;
S	is the Sutherland constant;
d	is the dimension of the spherical grains;
ε_1	is the emissivity of the grain surface;
C_0	is the Stefan–Boltzmann constant;
$\alpha = S_{abs}/(S_{c2} - L_2)$	is the integral coefficient of radiation absorption;
$S_{abs} = 2(L_2 - \Delta_2)\Delta_2 + \Delta_2$	is the area of radiation absorption in the elementary cell of second-order structure;
S_{c2}	is the area of the elementary cell in the second-order structure;
$\tau = \alpha l$	is the optical thickness of the medium.

LITERATURE CITED

1. A. F. Chudnovskii, Heat Transfer in Disperse Media [in Russian], GITTL, Moscow (1954).
2. W. Woodside and I. Messmer, J. Appl. Phys., 32, No. 9 (1961).
3. H. Godbee and W. Zeigler, J. Appl. Phys., 37, No. 1 (1966).
4. G. M. Kaganer, Thermal Insulation in Vacuum Engineering [in Russian], Mashinostroenie (1966).
5. G. N. Dul'nev and Z. V. Sigalova, Inzh. Fiz. Zh., 13, No. 5 (1967).
6. L. L. Vasil'ev and Yu. E. Frayman, Thermophysical Properties of Poor Heat Conductors [in Russian], Nauka i Tekhnika, Minsk (1967).

7. Z. V. Sigalova, "Investigation into the thermal conductivity of granular materials," Author's Abstract of Dissertation [in Russian], LITMO (1965).
8. V. Z. Bogomolov, Trudy Fiziko-Agronomicheskogo Instituta, No. 3, Leningrad (1941).
9. D. Kunii and I. Smith, AIChE Journal, 6, No. 1 (1960).
10. R. S Prasolov, "Investigation into heat transfer in a transient vacuum," Author's Abstract of Dissertation [in Russian], LITMO (1967).
11. A. S. Lyalikov, "The problem of thermal conductivity in granular materials," Author's Abstract of Dissertation [in Russian], Tomskii Politekhnicheskii Institut (1956).
12. A. A. Nekrasov, Zh. Tekh. Fiz., 10, No. 2 (1940).
13. W. Woodside, Can. J. Phys., 36, 815 (1958).
14. G. N. Dul'nev, Yu. P. Zarichnyak, and B. L. Muratova, Izv. Vuzov, Radiofizika, 9 No. 5 (1966).
15. L. L. Vasil'ev, "Structural thermophysics," Collection of Articles [in Russian], A. V. Luikov (editor), Energiya, Moscow–Leningrad (1966).
16. L. L. Vasil'ev, A. V. Luikov, A. G. Shashkov, and Yu. E. Frayman, Int. J Heat and Mass Transfer, 11, 117-140, Pergamon Press, London (1968).
17. G. N. Dul'nev, Inzh. Fiz. Zh., 9, No. 3 (1965).
18. G. N. Dul'nev and Yu. P. Zarichnyak, Inzh. Fiz. Zh., 12, No. 4 (1967).
19. G. N. Dul'nev and B. L. Muratova, Inzh. Fiz. Zh., 14, No. 1 (1968).